Scanning laser image correlation for measurement of flow

Molly J. Rossow
University of California, Irvine
Biomedical Engineering Department
3120 Natural Sciences 2
Irvine, California 92697-2715

William W. Mantulin
University of California, Irvine
Beckman Laser Institute
1002 Health Sciences Road
Irvine, California 92612

Enrico Gratton
University of California, Irvine
Biomedical Engineering Department
3120 Natural Sciences 2
Irvine, California 92697-2715

Abstract. Scanning laser image correlation (SLIC) is an optical correlation technique for measuring the fluid velocity of particles suspended in a liquid. This technique combines laser scanning of an arbitrary pattern with pair cross-correlation between any two points in the pattern. SLIC overcomes many of the limitations of other optical correlation techniques for flow measurement, such as laser speckle, spatial temporal image correlation spectroscopy, and two-foci methods. One of the main advantages of SLIC is that the concept can be applied to measurements on a range of scales through simple zooming or modifications in the instrumentation. Additionally, SLIC is relatively insensitive to instrument noise through the use of correlation analysis and is insensitive to background. SLIC can provide detailed information about the direction and pattern of flow. SLIC has potential applications ranging from microfluidics to blood flow measurements.
 [DOI: 10.1117/1.3365946]

Keywords: blood flow; image correlation; microfluidic channels; zebra fish.

Paper 09281R received Jul. 3, 2009; revised manuscript received Jan. 6, 2010; accepted for publication Jan. 15, 2010; published online Apr. 20, 2010.

1 Introduction

A wide range of disciplines, from surgery to cellular biology to microfluidics, need to measure the flow of small particles ranging from blood cells to proteins to cells. Optical correlation techniques can quantitatively measure flow.[1,2] These techniques are insensitive to detector noise through their use of correlation and relatively noninvasive through their use of light. Although there are a number of optical correlation techniques, they each have certain limitations in sensitivity and area of applications.

In this paper, we introduce scanning laser image correlation (SLIC), an optical correlation technique that has the potential to make measurements that are difficult or impossible with other techniques. In SLIC, a laser beam traces a pattern along or across a channel very rapidly with respect to the motion of the particles. By analyzing correlated fluctuations in the light that reflects back from the particles, we can extract the particles' velocities. SLIC uses a recently developed pair-correlation technique to analyze fluctuations.[3] With pair correlation, SLIC is capable of discriminating among multiple populations of particles traveling simultaneously through the same channel at different velocities. SLIC can also identify particles that have stopped moving and can detect spatial and temporal variations in velocity. The SLIC technique can make measurements quickly because the laser only scans points within the channel; regions outside the channel are ignored. Perhaps most importantly, the concept of SLIC can be applied to a range of applications on different scales. SLIC has the potential to make measurements in micron-sized regions of a cell and in blood vessels several centimeters long.

1.1 *SLIC: An Optical Correlation Technique*

Our preliminary evidence indicates that SLIC compares favorably to other optical-correlation velocity-measurement techniques, such as STICS, laser speckle, two-foci cross-correlation, and particle image velocimtery (PIV). Spatiotemporal image correlation spectroscopy (STICS) employs spatial correlation to measure flow.[2] STICS can be used to measure the velocity of fluorescently labeled proteins or unlabeled particles observed with reflected light.[2,4] In STICS, a series of images is acquired either through laser scanning or with a camera. Background subtraction is performed before correlation analysis to remove stationary objects. Image cross-correlation is performed between sequential images. Here, the temporal information comes from comparison between frames, not within each frame. STICS can be performed over a line instead of an image. STICS measures fluctuations that are slower than the frame or line time (typically, milliseconds to seconds).

STICS is limited in the range of velocities it can measure and in the spatial scales to which it can be applied. The maximum velocities that can be measured are limited by the frame rate of the camera or laser-scanning microscope.

Laser speckle is another optical technique to measure flow. In laser speckle, unlabeled particles are illuminated with a laser.[1,5] The light reflected off these particles produces an interference pattern that fluctuates as the particles move. The velocity of the particles can be extracted by analyzing this reflected light with temporal correlation and fitting the result

Address all correspondence to: Enrico Gratton, University of California, Irvine, Biomedical Engineering Department, 3120 Natural Sciences 2, Irvine, California 92697-2715. Tel: 949-824-2674; Fax: 949-824-1727; E-mail: egratton@uci.edu

1083-3668/2010/15(2)/026003/8/$25.00 © 2010 SPIE

with a mathematical model. Laser speckle can measure speed but does not provide the direction of flow of the moving particles. In its basic form, laser speckle provides a point measurement but it can be expanded to map flow through scanning. This is relatively slow because each point must be illuminated long enough to acquire sufficient statistics.

Two-foci cross-correlation is a flow-measurement technique that uses two laser beams (or one divided beam) focused at two separate points such that the focal volumes partially overlap.[6,7] Temporal correlation analysis is performed on the optical signals from the overlapping focal volumes. As particles move from one focal volume to another, the pattern of fluctuations changes. Like laser speckle, two-foci measurements must depend on a mathematical model to extract velocity from a pattern of fluctuations. Two-foci measurements are particularly unsuitable for application to larger scale problems because their sensitivity is dependent on the size and overlap of the focal volumes.

PIV is a technique that uses sheets of laser light to illuminate two planes in a stream of moving particles which are usually tracer particles.[8,9] PIV is used to monitor flow in both liquids and gas. A camera records the light reflected from the tracers particles in each illuminated plane, and correlation analysis is used to determine the average displacement between planes. PIV is a well-established technique that has been proven useful in many applications. Recently, it has even been adapted to be used in microfluidic channels.[10] However, the geometry of the optics for PIV limits its potential applications. The sheets of laser light are usually positioned perpendicular to the camera. This makes PIV, in its currently implementation, impractical for medical applications and multilayered microfulidics.

SLIC has the potential to overcome some of the limitations of existing optical correlation methods. It lends itself naturally to imagine because it is based on scanning, unlike speckle or two-foci measurements. SLIC does not require a mathematical model to measure velocity in a simple (i.e., laminar) flow pattern like laser speckle and the two-foci methods do. A mathematical model could be employed to explain SLIC measurements in a more complicated flow pattern. This feature of SLIC is discussed in greater detail in the theory section. SLIC is adept at following flow in circuitous channels, which are often encountered in biological systems (e.g., blood vessels). SLIC can be applied to greater range of size scales and velocities than STICS.

1.2 *SLIC Applications*

SLIC has many potential applications. We perform a series of simulations with SLIC to understand (*i*) basic results, (*ii*) multiple flow velocities, and (*iii*) detection of stationary particles. In this paper, we explore two applications in particular, microfluidics and blood flow measurements. Average flow through microfluidic channels can be controlled with a pump. However, SLIC can detect variations in the flow pattern within the channel caused by the shape of the channel and the performance of the pumping system. In this paper, we show SLIC measurements of flow through a variety of microfluidic channels. SLIC can also be used to measure blood flow by measuring the fluid velocity of blood cells. In this paper, a zebra fish model was used to verify the applicability of SLIC to blood flow measurements.

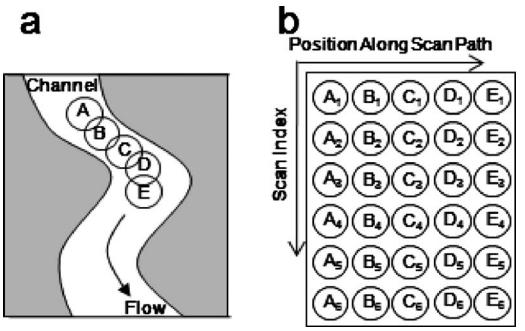

Fig. 1 In SLIC, a laser beam follows a trajectory across or along (as shown in the illustration) a channel. (a) The intensity of reflected light is recorded at a series of points along the scan path (not drawn to scale). The path is scanned many times, and each point in each scan is recorded as a pixel. The set of recorded pixels is displayed as (b) a two-dimensional plot, where the horizontal axis represents position in the trajectory and the vertical axis represents the sequence of trajectory scans. This type of plot is known as a carpet.

2 Theory

2.1 *SLIC Technique*

In SLIC measurements a laser follows a trajectory along or across a channel illuminating a series of small regions (defined by the focal volume of the laser) for several microseconds each, as is illustrated in Fig. 1(a). The reflected intensity from each region is measured with an optical detector. The path is scanned repeatedly, and a series of intensity measurements is collected at many points along the path.

Each SLIC measurement includes thousands of individual intensity measurements. The data can be displayed as a two-dimensional plot in which each intensity measurement is displayed as an intensity-scaled pixel, as illustrated in Fig. 1(b). In such a plot, the horizontal axis represents position in the trajectory and the vertical axis represents the sequence of trajectory scans. This type of plot is known as a carpet.

Even without further analysis, information can be obtained from the SLIC carpet. Moving particles, for example, will create diagonal lines with a slope related to the velocity. Stationary objects create vertical lines. Changes in velocity result in changing slopes in the diagonal lines. Quantitative information can be obtained by analyzing the data with the pair correlation technique described below.

2.2 *Pair Correlation*

Pair correlation analysis as used here was first described Digman and Gratton.[3] In that work, pair correlation was used to measure diffusion. Here we use the same computation to measure flow.

Information can be extracted from these data by calculating the cross-correlation between columns of the carpet. Each column is made up of intensity measurements from the same location. To measure velocity, we need to compare the position of a particle at one time to its position at a later time. Cross-correlation analysis allows us to make this comparison

statistically for all particles in each column. We use a normalized cross-correlation function defined as follows:

$$G_{ab}(\tau) = \frac{\langle \delta I_b(t) \cdot \delta I_a(t+\tau) \rangle_t}{(\langle I_a(t) \rangle_t \langle I_b(t) \rangle_t)}, \quad (1)$$

where I_a and I_b are the intensities values in columns a and b respectively. τ is the temporal correlation shift. $\langle\rangle_t$ is the temporal average and $\delta I(t) = I(t) - \langle I(t) \rangle$.

Paircorrelation is an application of cross-correlation that we use to analyze the SLIC carpet. In this analysis technique, cross-correlation is performed between two of the columns of the SLIC carpet. I_a is one column and I_b is another column. The "pair" in paircorrelation refers to pairs of columns separated by some distance.

Paircorrelation is useful for measuring fluid velocities. As particles flow from one point to another, they create fluctuations that are a fixed time apart. Paircorrelation extracts the time scale of these fluctuations and, therefore, the rate of flow.

Single-distance paircorrelation, paircorrelation calculated between all columns a fixed distance apart (columns 1 and 3, and columns 2 and 4, for example) can be used to analyze fluctuations due to flow. Single-distance paircorrelation can be visualized as a two-dimensional intensity plot, where each discrete point on the horizontal axis corresponds to a column pair, and the vertical axis is the time delay τ and color represents the magnitude of the correlation function. Example paircorrelation plots can be seen in the simulations section. This type of plot can be condensed to a one-dimensional plot that is also informative by averaging all the correlation curves. When the rate of flow is constant throughout the measurement and along the path scanned, we expect these cross-correlation curves to be similar except for noise. In both the two-dimensional plot, and the average plot the location of the correlation peak is dependent on the flow rate.

A simple, constant flow rate can be analyzed effectively with paircorrelation for a single distance. More complicated flow patterns are better analyzed using the complete range of possible distances between columns. Equation (2) defines pair correlation for multiple distances, d,

$$G(\tau, d) = \left\langle \frac{\langle \delta I(x,t) \cdot \delta I(x+d, t+\tau) \rangle_t}{(\langle I(x,t) \rangle_t \langle I(x+d,t) \rangle_t)} \right\rangle_d. \quad (2)$$

Multidistance paircorrelation can be depicted as a two-dimensional plot, where color represents the magnitude of the correlation and each column represents one pair of correlated columns from the original data. In this type of plot, the horizontal axis corresponds to the column pair index (the pair of columns correlated) and the vertical axis corresponds to τ. It is useful in visualizing paircorrelation to have a logarithmic scale on the vertical axis so that the lower τ values are emphasized.

A fitting function is not needed to interpret the multidistance pair-correlation plot. The correlation peak will have a slope that is related to the average velocity of the particles. Other features of the flow pattern will create distinctive features in this plot, as is discussed in more detail in Section 4. This is a strength of the SLIC method. It does not rely on mathematical models that make assumptions about the physics and optics of the system.

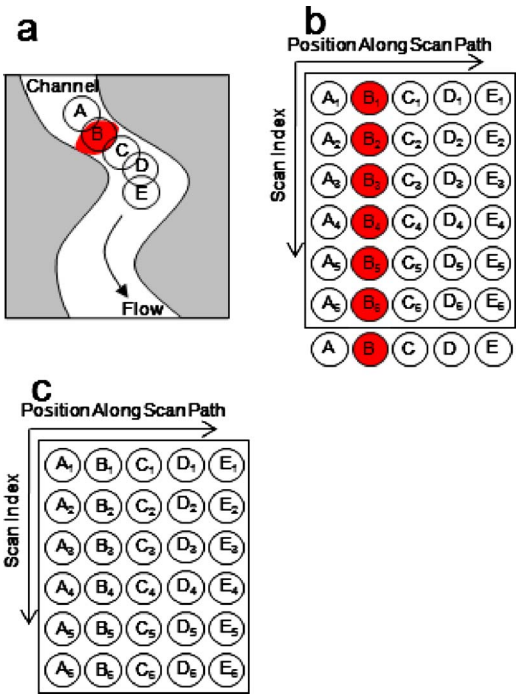

Fig. 2 Stationary object at location B creates a signal each time the path is scanned. (b) This creates a vertical line in the SLIC carpet. The average of all the rows of the carpet is subtracted from each row of the carpet to give (c) a version of the carpet with out vertical lines.

2.3 *Background Subtraction*

An additional computational step is performed before pair correlation to remove stationary objects from the line scan. Stationary objects, including the channel itself and particles that have become stuck to the channel wall, will create a signal at the same location in each scan as can be seen in Fig. 2(a). This will create a vertical line in the SLIC carpet [Fig. 2(b)]. Truly stationary objects, namely, objects that are fixed during the entire measurement time, will skew the correlation results and are not relevant to measuring the rate of flow. Instead particles that become stuck or that start to move if they were stuck are properly detected. The average of all the lines is subtracted from each line to remove the signal from truly stationary objects while preserving the signal from moving objects [Fig. 2(c)]. This has the result of removing the vertical lines (corresponding to stationary particles) from the SLIC carpet.

2.4 *Moving-Average Subtraction*

Particles that are temporarily stationary can also create signals that skew the correlation results and complicate interpretation of the SLIC carpet. These cannot be removed through background subtraction as described above. Instead of the average of *all* rows of the SLIC carpet, the average of only the subset of rows for which the particle remains stationary should be subtracted from each row of the carpet. We cannot know before analyzing the data exactly how long each particle remains stationary, but we can estimate and average a corresponding subset of rows. For each row, the subset of rows to average is different. For example, if the moving average window is five rows wide, then at row 20 rows, 15–25 will be

averaged. This approach will also remove a slowly moving background, such as that originated from the pulse or other slowly moving process.

3 Materials and Methods

3.1 *Simulations*

Simulations of flowing particles were performed and analyzed using the SLIC method. In these simulations, particles were represented as uniform disks moving in two dimensions. Fluid velocity was modeled as uniform displacement in the x direction at each time step, and boundary effects were ignored. Diffusion was modeled as pseudo-random displacements in the x and y directions. This pseudo-random displacement was generated from a normal distribution with a mean of zero and a standard deviation of $\sigma=\sqrt{2D\tau}$, where D was the diffusion coefficient in pixels^2/frame and τ is the frame time. Simulations were performed both under ideal conditions and with both shot noise and constant background. All simulations were performed using Matlab version 7.3.0.267 (R2006b) (Mathworks, Natick, MA).

The values of the parameters used in these simulations (expressed in terms of pixels) are as follows: each SLIC simulation used a scan-path 256 pixels long, and 1024 paths were scanned. The radius of the simulated particles was 2 pixels. The diffusion coefficient was 0.1 pixels^2/frame. The direction of flow was in the positive x direction as was the direction of scanning. Fluid velocity was varied from 0 to 15 pixels/scanpath. These values can be considered to model data acquired in the manner presented in this paper.

3.2 *Instrumentation*

In our experiments, we performed laser scanning with a Zeiss LSM 510 META-Confocor 3 laser scanning microscope (Carl Zeiss Inc., Germany) and with the Olympus FluoView FV1000. Light with a wavelength of 488 nm and a power of approximately 1–5 mW from an argon ion laser was used to scan the channels, and reflected light was detected using a photomultiplier tube. A 10X objective with a numerical aperture of 0.26 and a working distance of 30.5 mm was used to focus the laser. Because SLIC relies on comparing fluctuations at different locations, it is not sensitive to the size of focal volume, as long as the focal volume is small enough to. For measurements in single-channel microfluidics, each path scanned was a line 256 pixels long and the dwell time at each pixel was 3.21 μs. The scan time for each line was 1.93 ms, which includes additional time pausing at the beginning and end of each line. Each measurement included 8000 scans along the path. Measurements in multichannel microfluidics and zebra fish were performed using an appropriate number of pixels to include the length of the channel. For the multichannel microfluidics, 200 pixels were used. For the zebra fish, 100 pixels were used. For each measurement, the path was scanned 7000 times. This was far more scans than required to obtain an adequate signal-to-noise ratio but demonstrated that measurements could be performed on a time (in seconds). In the data presented here, a shorter range of path scans in shown to zoom in on features that occur on a shorter time scale. Using a laser-scanning microscope limited the sample to objects small enough to fit on a microscope stage. This technique could also be implemented with free-standing scanning mirrors and could then be applied *in vitro* and *in vivo*.

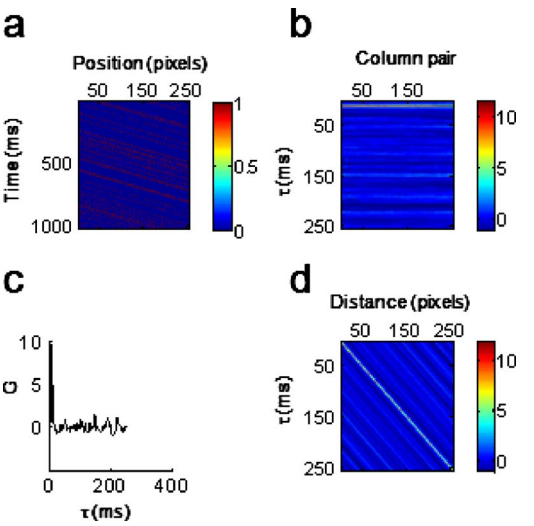

Fig. 3 Pair-correlation analysis performed on simulated SLIC data with a flow rate of 1 pixel/scan line: (a) The simulated carpet. Diagonal lines are caused by particles moving along the scan path. (b) The results of pair-correlation calculated at a distance of 10 pixels. A peak can be seen at τ=10 ms. (c) The average of all pair correlations at a distance of 10 pixels. Again, a peak is visible at τ=10 ms. (d) Two-dimensional plot of pair correlation calculated at distances 1–255. Here, there is a diagonal correlation peak.

3.3 *Microfluidic Channels*

The measurements were tested on microfrabricated channels obtained with photolithography as described by Jo et al.[11] Channels ranged from 100 to 250 μm wide. The depth of the channel was less precisely known due to a limitation of the fabrication processes but was ~50 μm deep. The channels were filled with a suspension of titanium dioxide (TiO_2, rutile) powder in water (Sigma-Aldrich, St. Louis, Missouri) with a concentration of 0.2 g/100 mL. The titanium dioxide particles included a range of sizes all <100 nm diam. The flow rate was controlled with a syringe pump (KDS100, KD Scientific, Holliston, Massachusetts). Flow rates ranged from 20 to 25 mL/h.

3.4 *Zebra Fish Measurement*

SLIC measurements were performed on zebra fish (*Danio rerio*) embryos to test SLIC in a physiological setting. Zebra fish were chosen because they have a well-characterized vascular system and are mostly transparent in the embryonic stage.[12,13] Three- to five-day-old zebra fish were immobilized in agarose gel during the measurements. All measurements where performed at room temperature, ~25°C. SLIC measurements were performed along various blood vessels in the tail, head, and abdomen.

4 Results

4.1 *Basic Simulations*

Representative results of the SLIC simulations are included in Fig. 3. The simulations were performed with a flow rate of

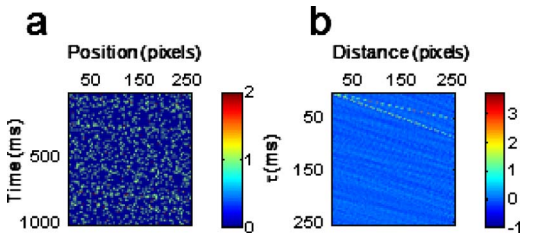

Fig. 4 Simulated carpet and SLIC analysis for two populations of particles moving at different velocities. (a) is the carpet plot of the simulated SLIC data. Each diagonal line is caused by an individual particle. (b) Pair correlation analysis. Two diagonal lines are caused by the two populations of particles with different velocities.

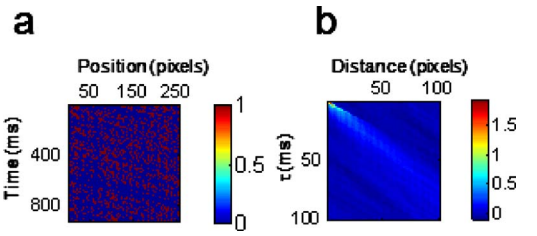

Fig. 5 SLIC simulation of particles that are temporarily stationary. In (a), the carpet plot, the stationary particles can be seen as vertical lines in the carpet. In (b), the correlation peak is widened by the stationary particles.

1 pixel/scan line. Figure 3(a) is the carpet plot of the simulated data. It contains diagonal lines, each caused by a moving particle that appears at a different position along the scan path for each scan. Figure 3(b) is a two-dimensional plot of all pair correlations at a distance of 10 pixels. As described above, the horizontal axis represented a pair of correlated columns from the original data. The vertical axis represents the temporal correlation shifts, and the color represents the magnitude of the correlation. A high-intensity horizontal band occurs at $\tau = 10$ ms. This is the correlation peak due to particles traveling at 1 pixel/line between 10 lines. Figure 3(c) is the average of all the columns of Fig. 3(b). Again, a peak can be observed at $\tau = 10$. This is a more condensed way of viewing the information in Fig. 3(b). Figure 3(d) contains the results of all pair correlations at distances from 1 to 255 pixels. As the distance between correlation pairs increases, the associated distance traveled by the particle increases as well. This is reflected in the diagonal line of high intensity seen in Fig. 3(d).

4.2 *Simulations with Multiple Velocities*

SLIC can distinguish between populations of particles traveling at different velocities in the same region. This can occur when the focal volume of the laser is large enough to include particles moving slowly close to the edge of the channel and particles moving faster closer to the middle of the channel. Figure 4 shows simulated SLIC data and pair correlation analysis for simulated data with two distinct velocities. In Fig. 4(a), the simulated SLIC data—two sets of diagonal lines with different slopes—can be seen. These are caused by the two different populations of particles moving at different velocities. The pair correlation analysis in Fig. 4(b) has two distinct correlation peaks, each with a different slope. These are also caused by the two populations of moving particles. The pair correlation plot includes additional diagonal lines with lower amplitudes. These are due to the initial placement of the particles. Because the amplitude is much lower, they can be ignored. They will decrease in intensity as the number of path scans increases in either a simulation or an actual measurement.

4.3 *Simulations with Temporarily Stationary Particles*

SLIC can also detect particles that temporarily become stationary. In the microfluidic channels described above, particles would occasionally stop moving for a period of time ranging from 10 to 1000 path scans. This may be due to particles catching on a rough surface of the channel. The experimental results are discussed in more detail later in the paper. Simulations of temporarily stationary particles were performed to determine the effect of stationary particles on the pair-correlation function calculation. Figure 5 shows carpet and SLIC calculations for simulated data with stationary particles. In Fig. 5(a) stationary particles can be observed as vertical lines throughout the image. In Fig. 5(b), the pair correlation at all distances has a correlation peak corresponding to the velocity of the moving particle. However, the plot is subtly altered by the temporarily stationary particles. At the origin, the correlation peak is elongated in the vertical direction and the entire correlation peak is widened.

4.4 *Microfluidics*

SLIC data are displayed as a two-dimensional plot in Fig. 6. Here, the first 256 path scans collected for fluid traveling at 25 mL/h are displayed. Vertical lines are visible in this plot and caused by stationary objects, possibly defects in the channel where titanium dioxide particles became stuck. These ob-

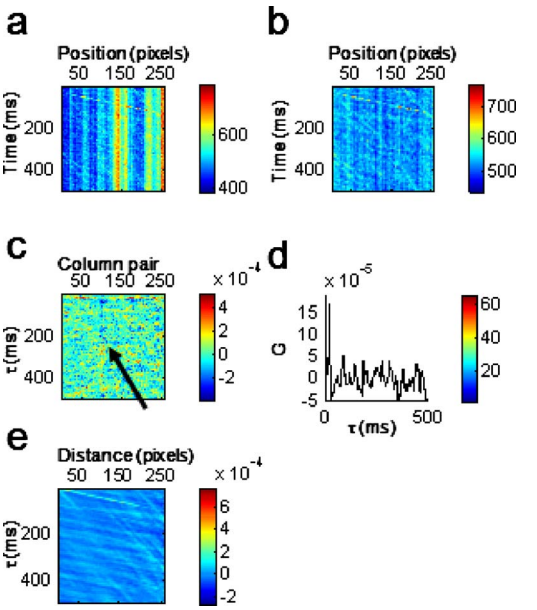

Fig. 6 (a) Carpet before background subtraction (b) the carpet after background subtraction, and (c) the correlations between columns at a column shift of 50 (The arrow points to the maximum correlation peak that can be observed in most but not all correlation columns), (d) the average pair correlation at a shift of 50, and (e) a two-dimensional plot of pair correlation performed at distances 1–255.

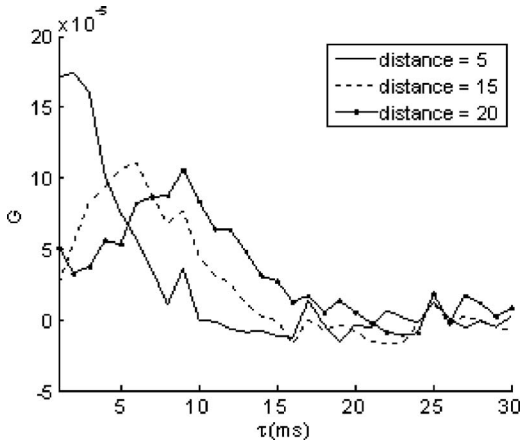

Fig. 7 Pair correlation between columns at varying distances. As the distance between columns increases, the correlation peak shifts to larger τ values.

jects are scanned every time the laser beam traces the path and appear in the same spot each time. There are also diagonal lines visible in Fig. 6(a). These lines are due to moving particles that are observed in "upstream" pixels in early scans and have moved to "downstream" pixels in later scans. These diagonal lines have a range of slopes, some steep, some shallow, indicating that particles are traveling at varying velocities. This is due to spatially varying velocities caused by surface effects in the channel. The focal volume defined by the scanning laser is large enough to include particles traveling slowly near the channels edge and faster closer to the channels center.

Figure 6(b) contains the same data as Fig. 6(a) but with stationary objects subtracted. Most of the vertical lines are no longer present because they have been subtracted out. The diagonal lines, the signal from moving particles, are still visible.

Figure 6(c) is a two-dimensional plot of pair-correlation analysis performed on the line scans from Fig. 6(a) at a spacing of 30 columns. A horizontal band of high light color (high magnitude) just above the center of the plot represents the correlation peak in most, but not all, of the correlated pairs of columns. Figure 6(d) is the average of the all the pair correlations displayed in Fig. 6(c). The correlation peak is still visible. Figure 6(e) contains the pair correlation at distance from 1 to 255 pixels. As in the simulated data, the correlation peak is a diagonal line and other features in the plot are of much lower amplitude. The strength of the pair correlation is that it incorporates all column pairs and does not rely on only two points that might not have a clear correlation peak or provide an accurate measurement.

Figure 7 contains the average pair correlation for the data presented in Fig. 6 at three different column distances. The correlation peak shifts to the right as the column spacing increases. Increasing the column spacing increases the distance the particle has traveled between columns and therefore increases the time it takes for the particle to travel between columns, which corresponds to the correlation peak appearing at a larger τ. The average velocity can be determined from this plot by determining the physical distance represented by the columns and dividing by τ at the peak correlation value.

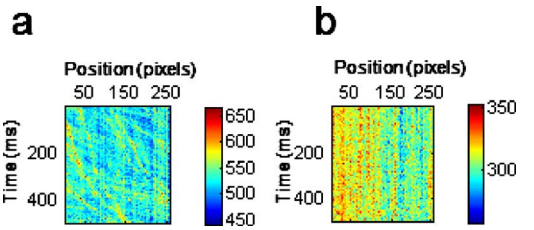

Fig. 8 Carpet data for a pump setting of 20 mL/h. Diagonal lines with different slopes can be observed as well as lines that change slope as the particles move from left to right. (b) is the SLIC carpet for a pump setting of 24 mL/h. Uneven vertical lines are caused by temporarily stationary particles. Both measurements were done using the same concentration of particles. However, uneven distribution of particles in the flow channel may make the number of particles that appear in each measurement different.

Information beyond average velocity is available from SLIC measurements. Multiple different velocities can be observed in the two-dimensional line-scanning plot as diagonal lines of varying slopes as can be seen in Fig. 4 and discussed above. Changes in velocity along the direction of flow can also be observed as particles slow down due to obstructions in the channel. Figure 8(a) is a carpet plot in which diagonal lines change slope as they move from left to right. On the left side of the image, these lines have shallow slopes indicating fast motion. On the right, the lines transition to a steeper slope indicating that the particles have slowed. Particles that are temporarily stuck can also be observed in SLIC data. Figure 8(b) shows SLIC data with the stationary objects subtracted. Some partly vertical lines remain. These indicate that there are particles that stick to the channel wall during several path scans but not for the entire time of data collection. This is most likely due to aggregates of TiO_2 the temporarily adhere to the channel walls. This could be particularly useful for studying medical conditions, such as atherosclerosis, where white blood cells accumulate on blood vessel walls.

4.5 *Branching Channels*

SLIC was also tested on channels that branch and curve. Figure 9(a) shows such a channel and the path that was scanned along it. Unlike the experiments presented above, the scan path is not a straight line but curved to follow the channel. Figure 9(b) shows the carpet from those scans. Sloping lines are present, each caused by the movement of an individual particle. The slopes of the lines are not constant across the carpet. The curving channel caused flow to be faster and slower at different locations, and the carpet reflects this variability in velocity.

4.6 *Zebra Fish*

A zebra fish model organism was used to test SLIC in a physiological environment. The tail of the zebra fish was examined, as shown in Fig. 10(a). Two scans were performed: one along a blood vessel and one in a region of tissue where no blood vessel was present. The carpet from this series of scans is shown in Figs. 10(b) and 10(c). For the scan along the blood vessel, the rate of flow fluctuates with the heart pulse rate of the fish. No flow can be seen in the scan where there is no blood vessel. Although there is no blood flow in this part of

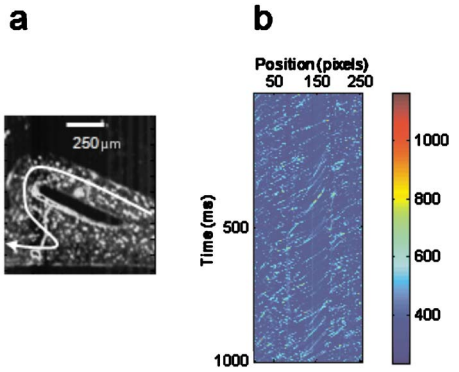

Fig. 9 (a) Microfluidic channel filled with a flowing liquid. The white arrow is the scan path. The direction of flow is left to right. The channel curves and branches causing the rate of flow to change at different locations in the channel. (b) The carpet data from those scans. Lines from the moving particles are present, but the slope changes across the image.

the zebra fish tail, it is likely that the pulse causes some movement in the tissue. This will not have the same appearance as flow in the SLIC carpet because the motion will be localized and not regular over the entire length of the scan. The average velocity of the blood can be extracted determining the slope of these scans and averaging over a range of heart beats. The results of this analysis is presented in Fig. 10(d).

5 Discussion

5.1 *Technical Considerations*

Accurate SLIC measurements are subject to certain limitations and technical requirements. The duration of a single scan must be shorter than the time a particle takes to move the distance of the scan or the particle will only appear on one scan and no statistical comparison can be made between locations along the path. The duration of a single scan is dependent on the number of points scanned and the dwell time at each pixel, while the length of a single scan depends on the zoom used in the microscope. Scan rates can be increased by decreasing the pixel dwell time. This may be appropriate for scanning fast flow rates over large areas. Because in the microscope the duration and length for a scan can be made independent of the number of pixels acquired along the scan, this method will never miss local flow patterns that occur between pixels. In the shorter length scale, the method is limited by the size of the laser beam, which is diffraction limited in the microscope. SLIC can also be used to measure pure diffusion. In this case, the distance traveled by a particle will depend on the square root of time.

5.2 *Additional Applications*

In this paper, SLIC was used to measure the fluid velocity of blood in a simple animal model. SLIC could also be used to measure the fluid velocity of blood in exposed blood vessels during surgery in humans or in an animal model. More development is needed to bring SLIC technology to this point. The laser-scanning system must be modified to be free standing and not microscope based. Scattering from the tissue will decrease the signal-to-noise ratio and must be accounted for. However, if this system can be implemented, then it would provide detailed information on localized blood flow and could be useful for studying conditions that interfer with blood flow, such as atherosclerosis and malaria.

We have also demonstrated the utility of SLIC for performing measurements in microfluidic channels. Microfluidics are another potential application of SLIC measurements. One application of microfluidics is to facilitate microscale chemical reactions by mixing two or more fluids. Mixing in microfluidics is a challenge because it is difficult to create turbulent flow in microscale channels. In some microfluidics designs, mixing is based entirely on diffusion.[14] Understanding the flow rate is important is to determining the speed of mixing and the rate of the reaction. Other microfluidic devices attempt to generate chaotic flow patterns. In these channels, it is important to measure not only the average flow rate but also to identify where turbulence occurs and under what condi-

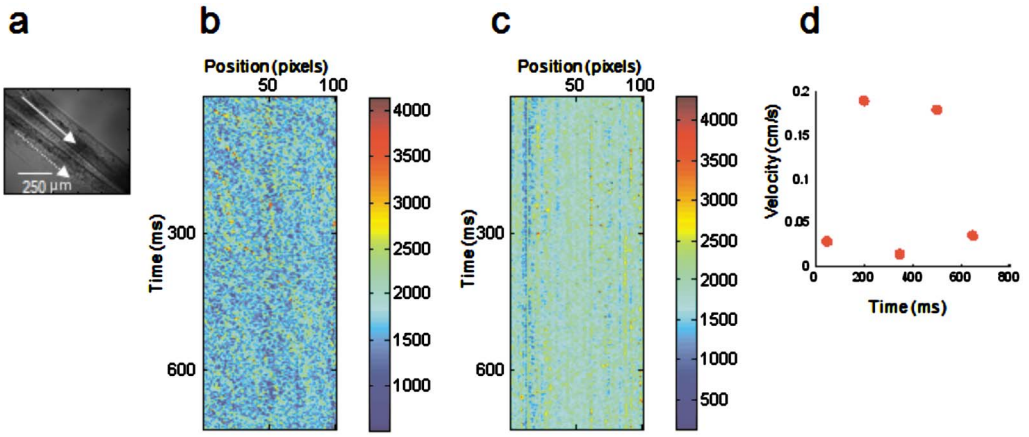

Fig. 10 (a) Tail of a zebra fish larvae. The solid white arrow indicates the location and direction of the first scan, along a blood vessel. The scan was performed to measure flow through a blood vessel running along the tail of the fish. (b) The carpet plot for a series of scans—a series of curving, approximately diagonal lines can be seen in the carpet. The slope of the line changes with the heart rate of the fish. (c) The SLIC carpet from a scan along the dashed line in (a). There is no blood vessel here, and no flow can be seen in the carpet. (d) shows the blood velocities extrapolated from the slope of lines in the SLIC carpet (b).

tions. SLIC can provide information about flow through both types of mixing channels.

Microfluidic devices are also used to create a controlled environment in which to grow cell cultures.[15] The exact amount of nutrients, growth factors, and other parameters can determine whether or not cells thrive or the success of a particular experiment. Controlling fluid velocity is necessary to ensure that the correct quantities of these substances reach the cells at the correct times. SLIC could be used to test the rate of flow through an entire microfluidic system.

Vascular cell culture and tissue engineering of vascular grafts with microfluidics is an area in which fluid velocity measurements are particularly useful. Vascular cell growth patterns respond to sheer stress, which is dependent on fluid velocity.[16] Microfluidic channels for vascular design can be quite complex, and it can be useful to measure the fluid velocity through the entire network of channels. This could be accomplished efficiently with SLIC.

6 Conclusions

SLIC can measure flow through small channels. It is fast and efficient because it only records data from areas where there is actually flow and does not scan outside channels. This technique can provide the average rate of flow along the path as well as localized flow rates and identify temporarily stationary particles. Additionally, SLIC can be expanded to scan over complex flow patterns and applied to measurements of blood flow or flow through microfluidic channels.

Acknowledgments

This research was supported by the National Institutes of Health (Grant No. *PHS 5 P41-RR003155*.) The authors also acknowledge Thomas Schilling and his lab for providing the zebra fish.

References

1. J. D. Briers and A. F. Fercher, "Retinal blood-flow visualization by means of laser speckle photography," *Invest. Ophthalmol. Visual Sci.* **22**(2), 255–259 (1982).
2. B. Hebert, S. Costantino, and P. W. Wiseman, "Spatiotemporal image correlation spectroscopy (STICS) theory, verification, and application to protein velocity mapping in living CHO cells," *Biophys. J.* **88**(5), 3601–3614 (2005).
3. M. A. Digman and E. Gratton, "Imaging barriers to diffusion by pair correlation functions," *Biophys. J.* **5** 665–673 (2009).
4. M. J. Rossow, W. W. Mantulin, and E. Gratton, "Spatiotemporal image correlation spectroscopy measurements of flow demonstrated in microfluidic channels," *J. Biomed. Opt.* **14**(2), 024014 (2009).
5. D. J. Briers, "Laser Doppler, speckle and related techniques for blood perfusion mapping and imaging," *Physiol. Meas* **22**, R35–R66 (2001).
6. J. Enderlein and R. A. Keller, "Comparison of one-focus and two-foci setup in single-molecule detection experiments," *Appl. Spectrosc.* **51**(3), 443–446 (1997).
7. J. E. Martin Böhmer, "Fluorescence spectroscopy of single molecules under ambient conditions: methodology and technology," *ChemPhysChem* **4**(8), 792–808 (2003).
8. I. Grant, "Particle image velocimetry: a review," *Proc. Inst. Mech. Eng., Part C: J. Mech. Eng. Sci.* **211**(1) (1997).
9. J. Bolinder, *On the accuracy of a digital particle image velocimetry system*, pp. 1–24, Lund Institute of Technology, Lund, Sweden (1999).
10. R. Lima, S. Wada, K.-I. Tsubota, and T. Yamaguchi, "Confocal micro-PIV measurements of three-dimensional profiles of cell suspension flow in a square microchannel," *Meas. Sci. Technol.* **17**, 797 (2006).
11. B.-H. Jo, L. M. Van Lerberghe, K. M. Motsegood, and D. J. Beebe, "Three-dimensional micro-channel fabrication in polydimethylsiloxane (PDMS) elastomer," *J. Microelectromech. Syst.* **9**(1), 76–80 (2000).
12. A. S. Forouhar, M. Liebling, A. Hickerson, A. Nasiraei-Moghaddam, H.-J. Tsai, J. R. Hove, S. E. Fraser, M. E. Dickinson, and M. Gharib, "The embryonic vertebrate heart tube is a dynamic suction pump," *Science* **312**, 751–753 (2006).
13. N. V. Iftimia, D. X. Hammer, R. D. Ferguson, M. Mujat, D. Vu, and A. A. Ferrante, "Dual-beam Fourier domain optical Doppler tomography of zebrafish," *Opt. Express* **16**(18), 13624–13636 (2008).
14. H. Wang, P. Iovenitti, E. Harvey, and S. Masood, "Optimizing layout of obstacles for enhanced mixing in microchannels," *Smart Mater. Struct.* **13**(6), 662–667 (2002).
15. J. T. Borenstein, H. Terai, K. King, E. J. Weingberg, M. R. Kaazemput-Mofrad, and J. P. Vacanti, "Microfabrication technology for vascularized tissue engineering, *Biomed. Microdevices* **4**(3), 167–175 (2002).
16. S. Levenberg, "Engineering blood vessels from stem cells: recent advances and application," *Curr. Opin. Biotechnol.* **16**(5), 16–253 (2005).